

1 **Supporting Information for ”Large-scale drivers of**
2 **tropical extreme precipitation events: the example of**
3 **French Overseas Territories”**

E. Cornillault¹, P. Peyrille¹, F. Couvreur¹, and R. Roehrig¹

4 ¹Centre National de Recherches Météorologiques, Université de Toulouse, Météo-France, CNRS, Toulouse, France

5 **Contents of this file**

6 1. Texts S1 to S2

7 2. Figures S1 to S12

Introduction

8 The supplementary information:

9 • illustrates the topography of each territory (Text S1 and Figure S1)

10 • documents the methodological approach to assess the statistical significance of our
11 results (Text S2);

12 • shows the geographical spread of the rain-gauge network of each territory, together
13 with the 99th percentile of each station (Figure S2);

14 • provides the sensitivity analysis of the fraction of cyclonic EPEs regarding the max-
15 imum distance between TCs and rain gauges (Figure S3);

16 • illustrates the sensitivity of cyclonic EPEs to the distance threshold used to define
17 cyclonic days (500 km and 1500 km in Figures S4 and S5, respectively);

18 • documents the TC contribution to rainfall (a), the fraction of cyclonic days in the
19 whole period study (b), and the average rainfall during a cyclonic day (c) (Figure S6);

20 • indicates at the scale of each rain gauge the difference in mean intensity between
21 cyclonic and non-cyclonic EPEs (Figure S7);

22 • exhibits the large-scale patterns (OLR, PW, and 850-hPa wind anomalies) associated
23 with non-cyclonic EPEs for Mayotte, French Guiana, Martinique, New Caledonia, Wallis
24 & Futuna, Society islands, Marquesas islands and Gambier islands (Figures S8 and S9);

25 • shows the PDFs of 850-wind direction for all days and the wind direction of anomalies
26 during non-cyclonic EPEs (Figures S10 and S11).

27 • documents the contribution of the different time scales to the OLR anomaly associ-
28 ated with non-cyclonic EPEs (Figure S12).

Text S1: Geographic details about territories and rain gauges

29 Most of the islands studied have significant topographic features. The highest point
 30 is in Reunion (3050m, Piton des Neiges), and many mountains are over 2000m on the
 31 same island. Tahiti is the second-highest island, with a mountain reaching 2241m (Mount
 32 Orohena). Then came New Caledonia (with mountain ranges reaching 1618m with the
 33 Mount Humboldt), Martinique, and Guadeloupe, with mountains between 1000m and
 34 1500m, such as in Society Islands (except Tahiti). Marquesas islands are just a degree
 35 below, with mountains of 900m to 1000m. French Guiana has several mountains reaching
 36 600 to 800m. Finally, reliefs in St-Barthelemy, Mayotte, Wallis & Futuna, Gambier, and
 37 Austral islands reach only several hundred meters. Tuamotu archipelago is only composed
 38 of atolls with no significant relief.

Text S2: Significance tests

39 This section describes how the statistical significance of results in Figures 2c, 3, 4, S3c,
 40 S4c, S6, and S7 is determined. Statistical significances of the change in EPE probability
 41 (Figures 2c, S3c, S4c) and composite maps (Figures 3, S6, and S7) are adapted from the
 42 study of Peyrillé et al. (2023).

Change in cyclonic EPE probability

43 The statistical significance of the change in cyclonic EPE probability ($\Delta P_{EPE,c}$, defini-
 44 tion in Section 2.2) is tested against the null hypothesis corresponding to random EPE
 45 occurrence with respect to cyclonic days, with a bootstrap approach (Efron, 1979). N_r is
 46 the number of rain gauges for each territory. The number of cyclonic days N_c associated

with a given TC category is first computed from the climatology for each rain gauge.

Then, 1000 random samples are generated as follows:

1. a rain gauge of the territory is randomly selected, and an ensemble of N_c dates are randomly sampled among all the days of the studied period, with replacement;
2. the number of EPEs within this ensemble of N_c dates is then computed, and the change in EPE probability is deduced from this number of EPEs obtained previously.
3. the two previous steps are repeated N_r times by selecting a new rain gauge with replacement. The average over the N_r change in EPE probability provides the value of $\Delta P_{EPE,c}$.

The computed 1000 $\Delta P_{EPE,c}$ describes the $\Delta P_{EPE,c}$ distribution for the null hypothesis of the given territory and the given TC category. The change in EPE probability is finally considered statistically significant at the 95% confidence level when it is either larger than the 97.5th percentile or smaller than the 2.5th percentile of this $\Delta P_{EPE,c}$ distribution. These thresholds are displayed by vertical bars in Figures 2c, S3c, and S4c.

Composite maps of non-cyclonic EPEs

The statistical significance of the non-cyclonic EPE composite mean is assessed with a bootstrap approach. The null hypothesis is that large-scale conditions associated with EPEs are ordinary in climatology. As previously, N_r is the number of rain gauges within a given territory, and, for each rain gauge, we have $N_{EPE_{nc}}$ the number of non-cyclonic EPEs (as defined in Section 2.3, noted here EPE_{nc}). We then define Non- EPE_{nc} for each rain gauge as all the dates with the same day and month as EPE_{nc} for all years between 1979 and 2021 that are not non-cyclonic EPEs. The bootstrap approach follows:

:

68 1. a rain gauge is randomly selected, and an ensemble of $N_{EPE_{nc}}$ dates are sampled
 69 among all the EPE_{nc} and Non- EPE_{nc} dates, with replacement;

70 2. the composite for the rain gauge is computed by averaging the data over the previous
 71 ensemble of dates.

72 3. the two previous steps are repeated N_r times by selecting a new rain gauge replace-
 73 ment. The average over the N_r rain gauge provides a null composite.

74 The computed 1000 null composites describe the composite distribution for the null
 75 hypothesis. Then, for each data grid point, the statistical significance of the EPE_{nc}
 76 composite mean is evaluated against this null distribution using a two-tailed test at the
 77 95% confidence level. Only significant values are shown in Figures 3, S6, and S7.

PDFs during non-cyclonic EPEs

78 PDFs of atmospheric parameters during EPE_{nc} (Figure 4 and S8) are compared with
 79 the same PDF but for non- EPE_{nc} dates using a Mann–Whitney U test (Mann & Whitney,
 80 1947). This test compares the combined rank of the values of both PDFs, supposed to be
 81 independent, to determine which is greater than the other. The following hypotheses are
 82 tested with a one-tailed test:

- 83 • H_1 , the EPE_{nc} PDF is higher for PW (lower for OLR) than the Non- EPE_{nc} one;
- 84 • the null hypothesis H_0 , the EPE_{nc} PDF is not higher for PW (lower for OLR) than
 85 the Non- EPE_{nc} one.

86 If the p -value is inferior to 0.05 (95% confidence level), H_1 is considered valid and
 87 distributions are significantly different. This significance diagnostics is performed for
 88 each rain gauge. Almost all EPE_{nc} PDFs (for PW and OLR and their anomalies) are

89 significantly different from the non-EPE_{nc} PDFs (not shown), indicating that averaged
90 PDFs can also be considered significantly different (superior for PW and inferior for OLR)
91 from those derived from the Non-EPE_{nc} dates. The same diagnostics computed against
92 climatological PDFs also indicate significantly positively (negatively) skewed PW (OLR)
93 PDFs during non-cyclonic EPEs.

References

- 94 Efron, B. (1979). Bootstrap Methods: Another Look at the Jackknife. *The Annals of*
95 *Statistics*, 7(1), 1–26. doi: 10.1214/aos/1176344552
- 96 European Space Agency, & Sinergise. (2021). *Copernicus Global Digital Surface*
97 *Model*. OpenTopography. Retrieved 2024-06-11, from [https://opentopography](https://opentopography.org/meta/OT.032021.4326.1)
98 [.org/meta/OT.032021.4326.1](https://opentopography.org/meta/OT.032021.4326.1) doi: 10.5069/G9028PQB
- 99 Mann, H. B., & Whitney, D. R. (1947). On a Test of Whether one of Two Random Vari-
100 ables is Stochastically Larger than the Other. *The Annals of Mathematical Statistics*,
101 18(1), 50–60. doi: 10.1214/aoms/1177730491
- 102 Peyrillé, P., Roehrig, R., & Sanogo, S. (2023). Tropical Waves Are Key Drivers of
103 Extreme Precipitation Events in the Central Sahel. *Geophysical Research Letters*,
104 50(20), e2023GL103715. doi: 10.1029/2023GL103715
- 105 Welch, B. L. (1947). The generalization of ‘Student’s’ problem when several different
106 population variances are involved. *Biometrika*, 34(1-2), 28–35. doi: 10.1093/biomet/
107 34.1-2.28

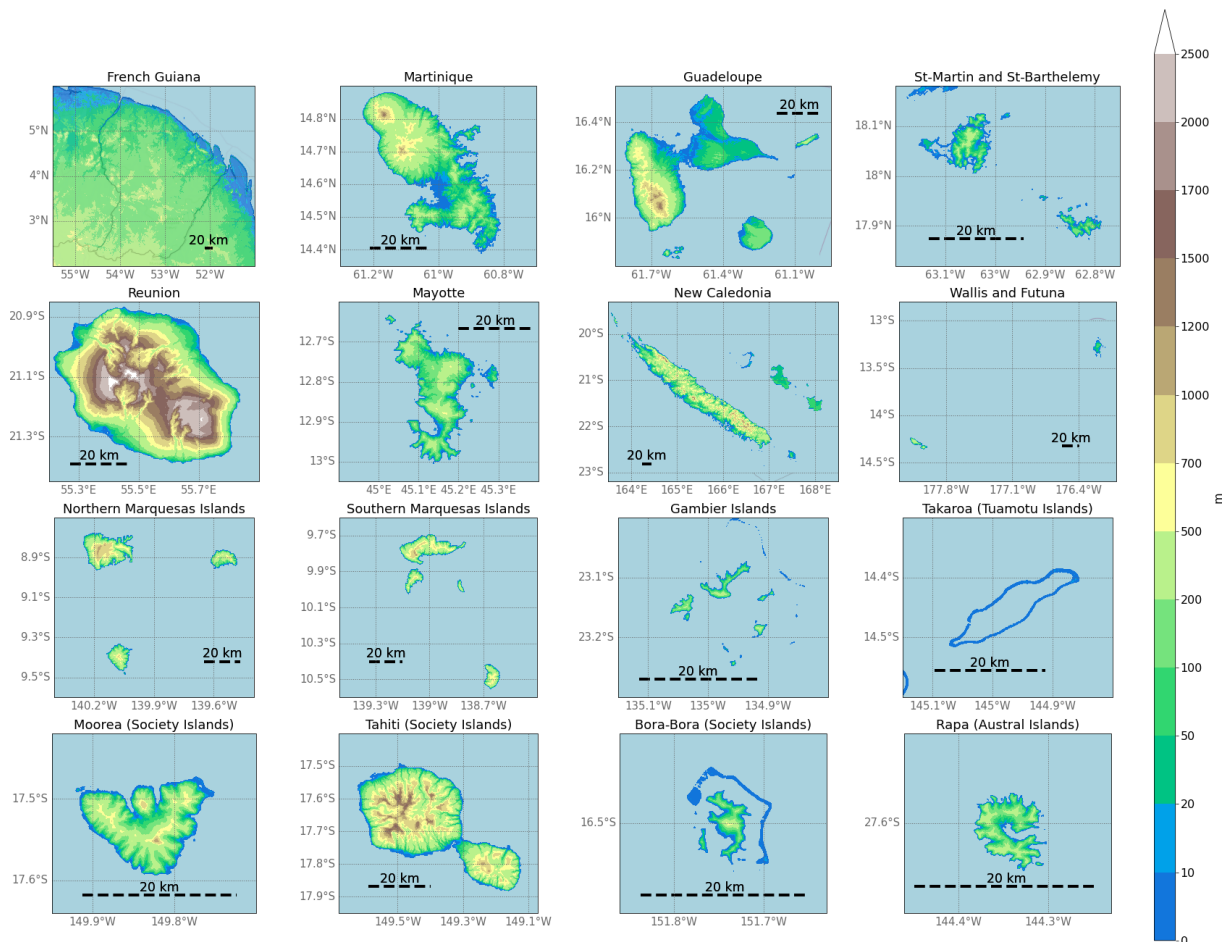


Figure S1. Topographic maps of the French Overseas Territories involved in the study (where at least one rain gauge can be found). A map scale of 20 km is indicated in each subplot. Data were extracted from OpenTopography (European Space Agency & Sinergise, 2021)

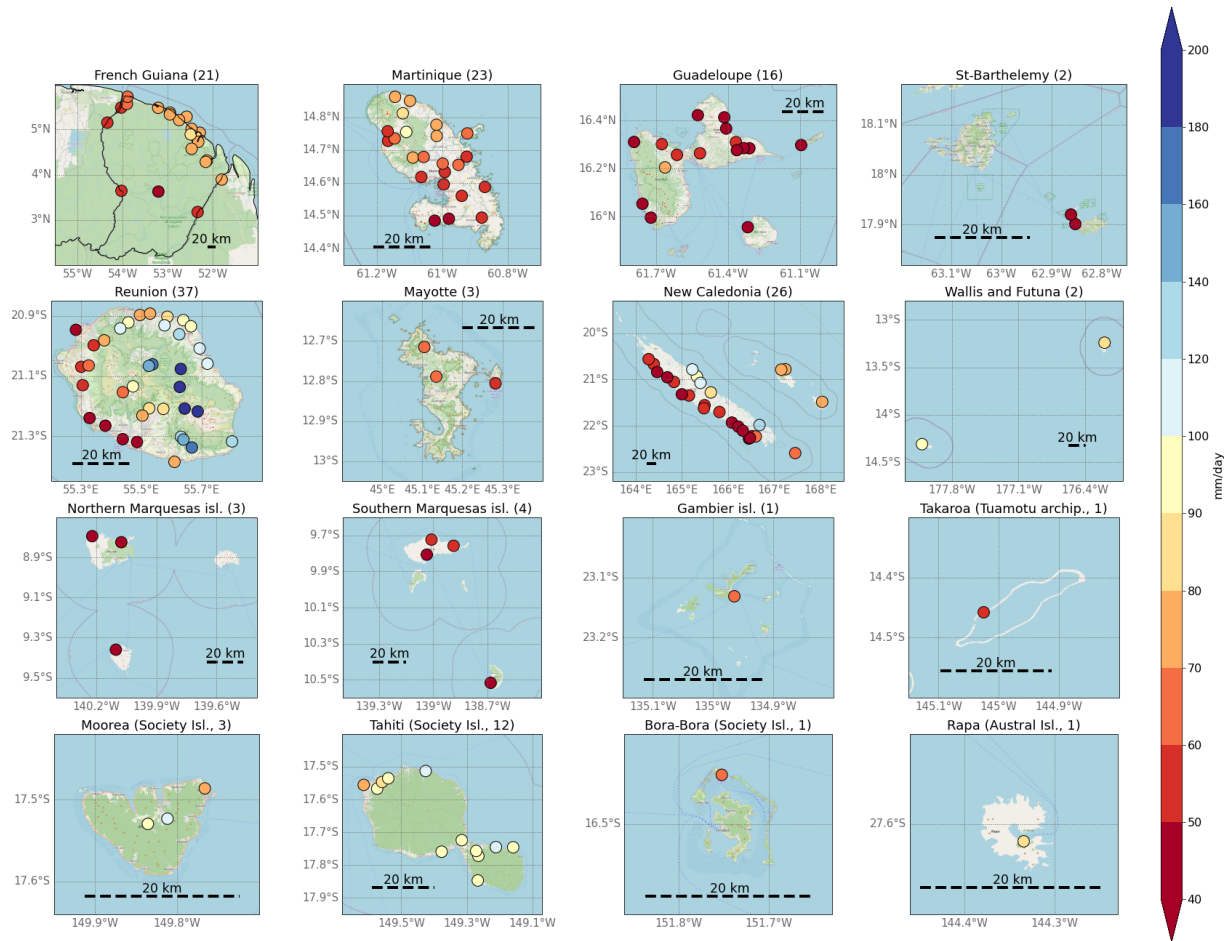


Figure S2. 99th all-day rainfall percentile (in mm day^{-1}) of each rain gauge for each territory network used in our study (number of rain gauges indicated in each panel title in brackets).

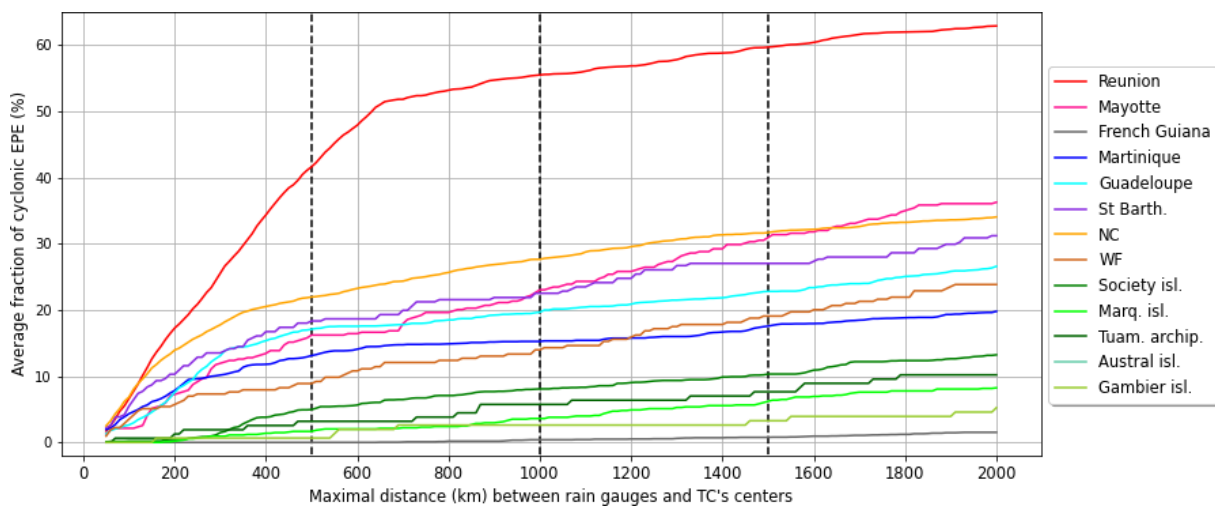


Figure S3. Fraction of cyclonic EPEs averaged over the rain gauges of each territory as a function of the threshold distance used to attribute an EPE to a TC. The distance corresponds to the maximum distance between the rain gauge and the TC center. Thresholds of 500, 1000, and 1500 km chosen for sensitivity assessment (Figures 2, S4, and S5) are indicated by vertical black dashed lines.

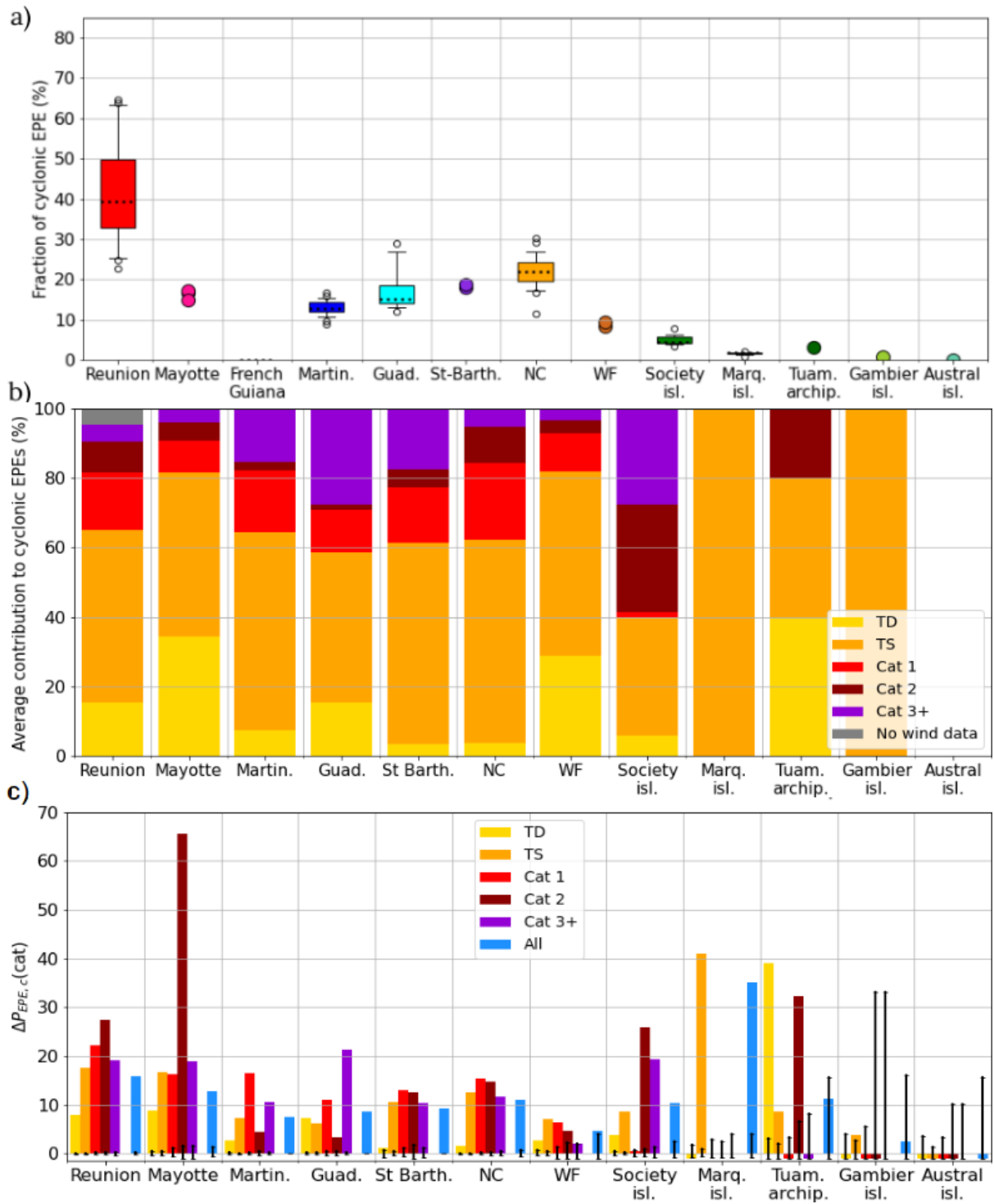


Figure S4. Same as Figure 2 but defining cyclonic days and cyclonic EPEs with a 500-km threshold

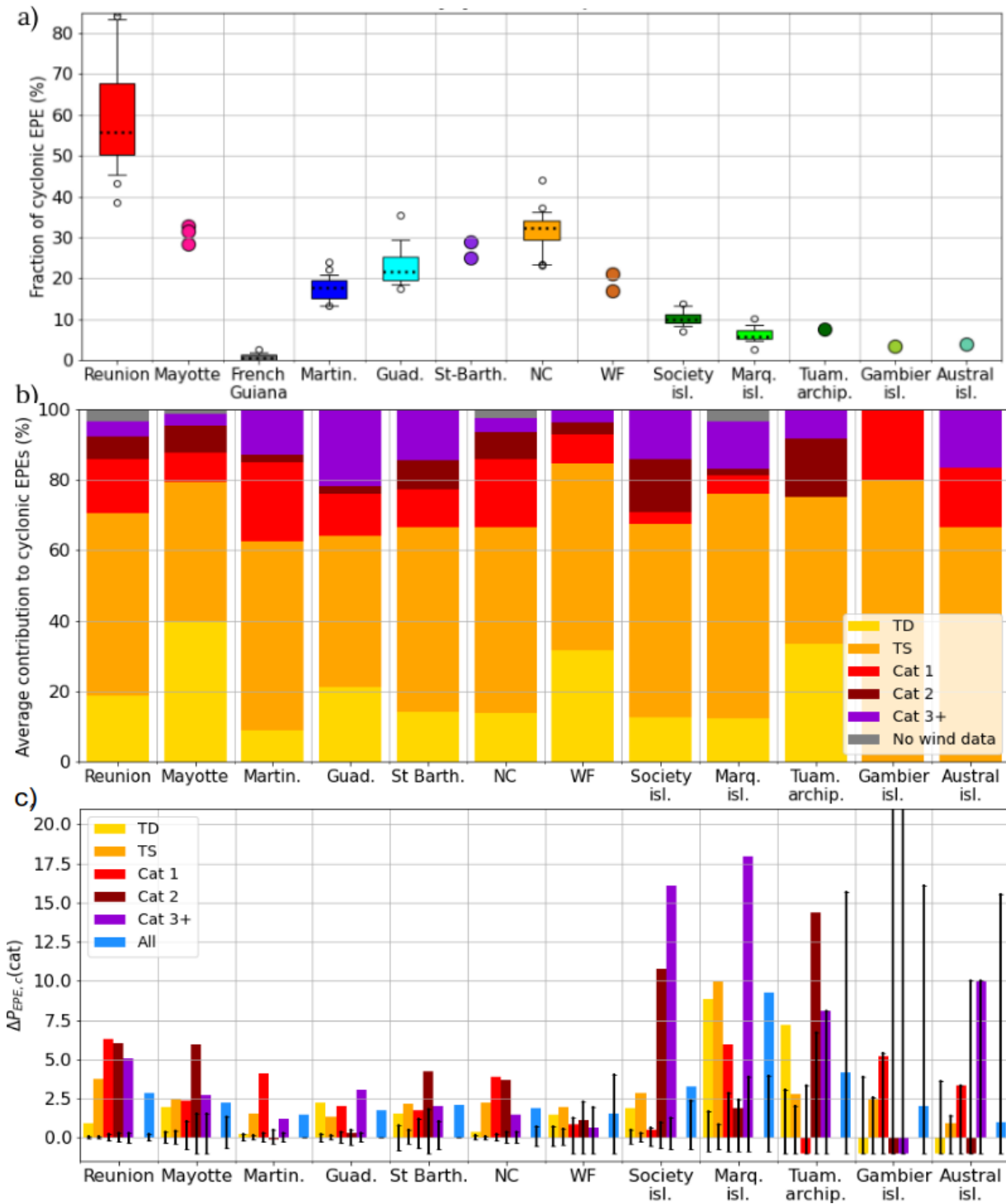


Figure S5. Same as Figure 2 but defining cyclonic days and cyclonic EPEs with a 1500-km threshold

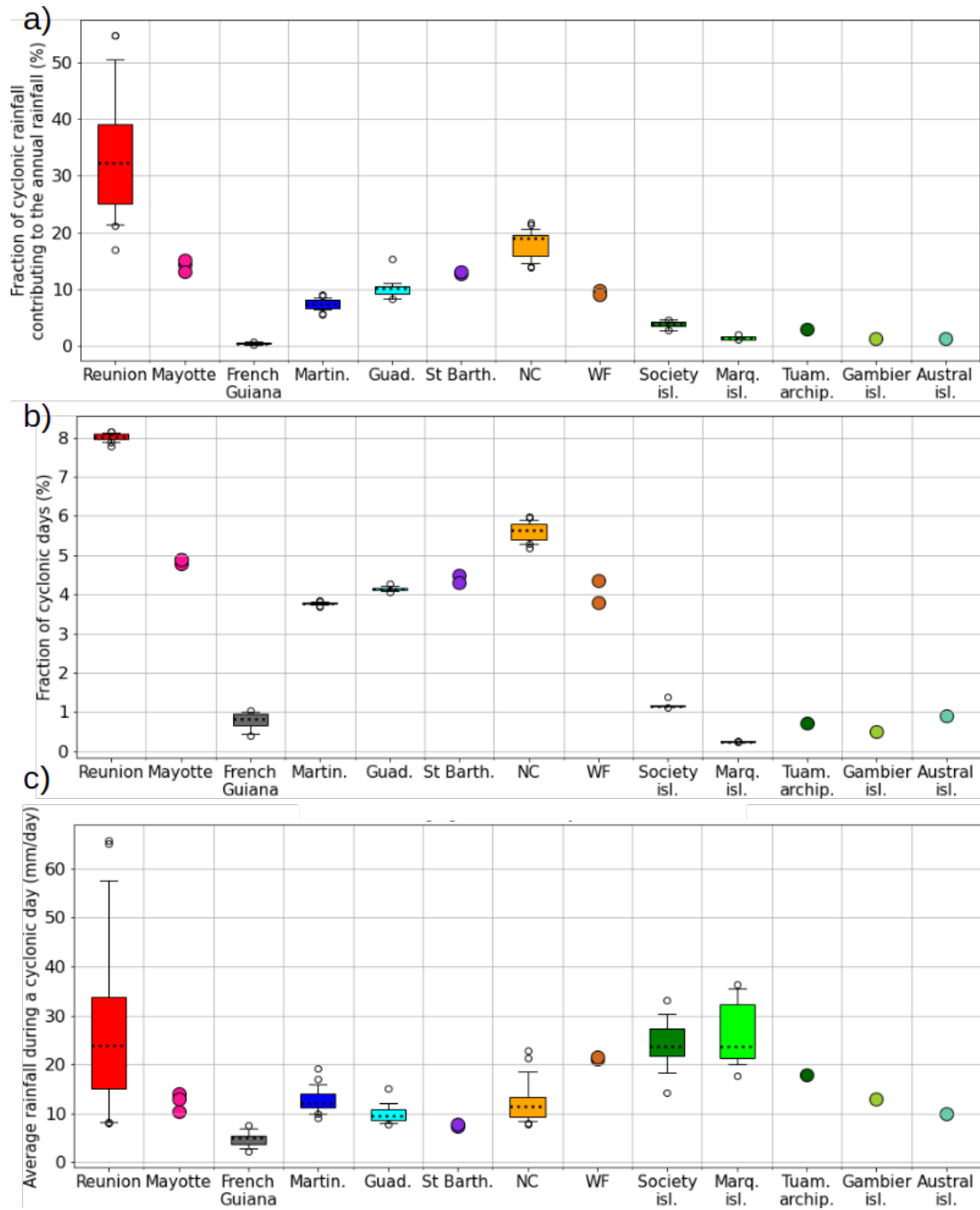


Figure S6. For each territory, distribution across its rain-gauge network of the TC contribution to rainfall (a), the fraction of cyclonic days in the whole period study (b), the fraction of cyclonic days among rainy days (more than 1mm/day) (c), and the average rainfall during a cyclonic day (d) (same boxplots as in Fig 1).

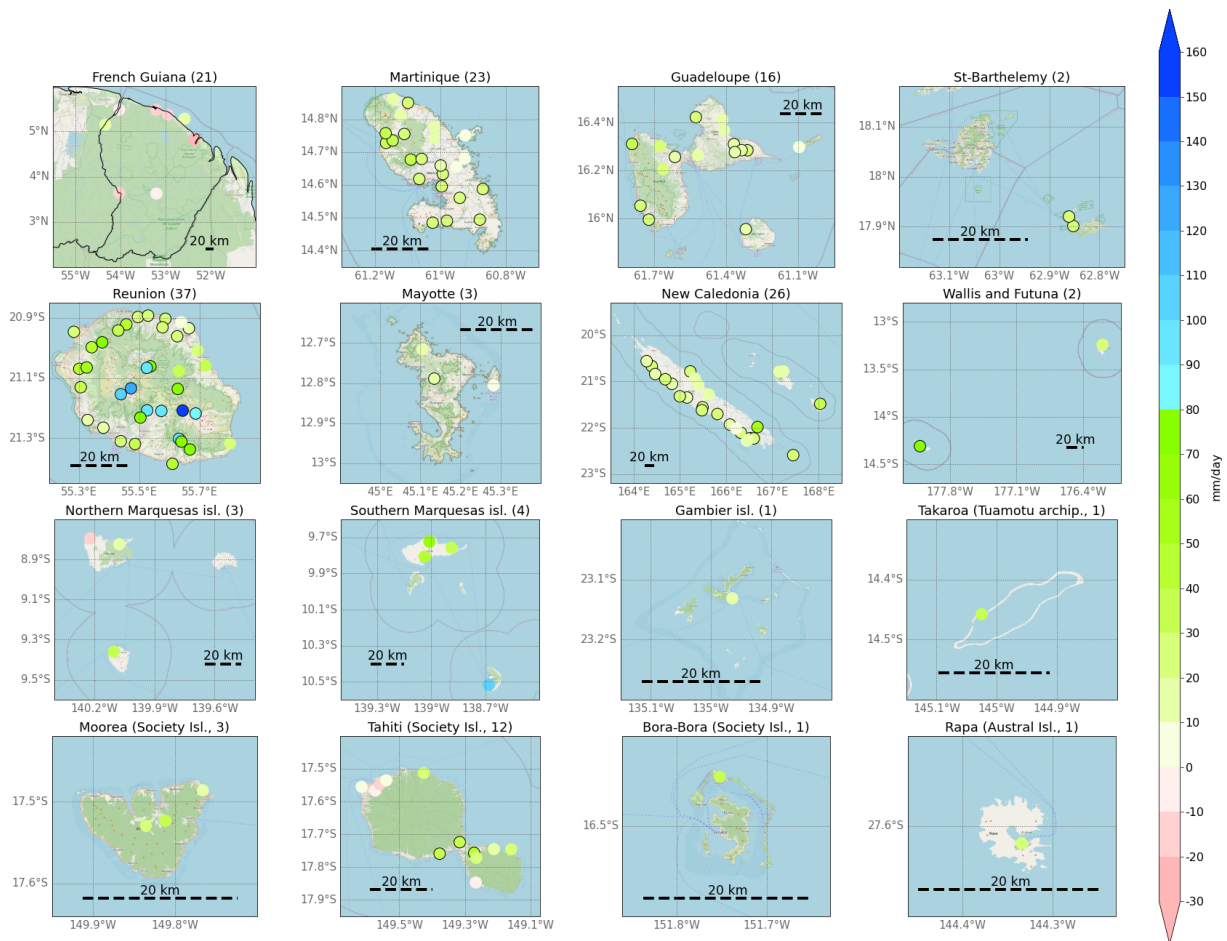


Figure S7. Mean rainfall amounts (in mm day⁻¹) difference between cyclonic and non-cyclonic EPEs. Rain gauges with a black circle indicate that the difference is significant at the 95% confidence level according to a Welch's t-test (Welch, 1947).

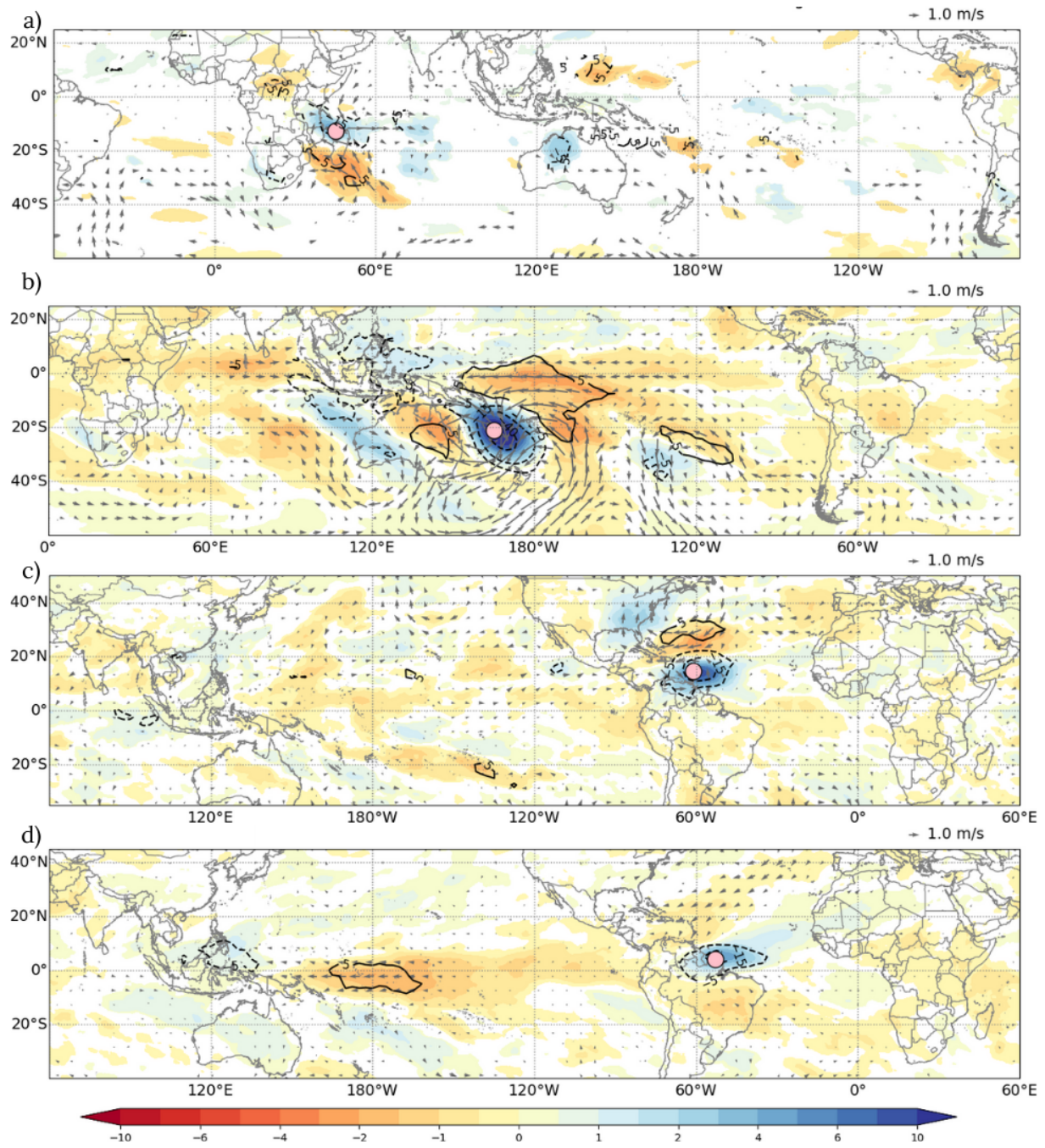


Figure S8. Same as Figure 3a but for other territories: Mayotte (a), New Caledonia (b), Martinique (c), and French Guiana (d). Composite maps for Guadeloupe and St-Barthelemy are similar to Martinique (not shown).

July 1, 2024, 7:40pm

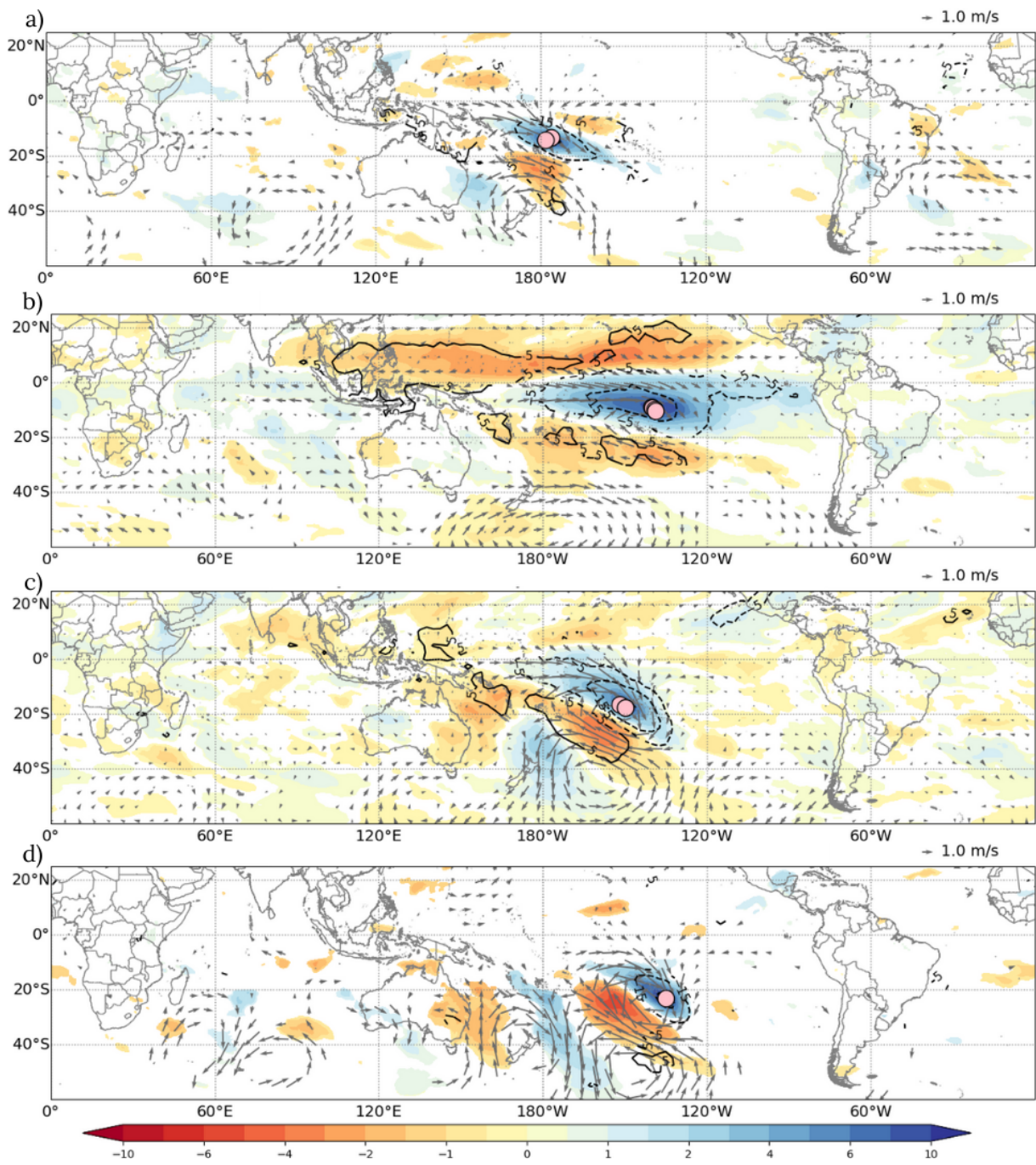


Figure S9. Same as Figure 3a but for other territories: Wallis & Futuna (a), Marquesas islands (b), Society islands (c), and Gambier islands (d). The map for the Tuamotu Islands is similar to the Society Islands, and the composite map of the Austral Islands is similar to the Gambier Islands (not shown).

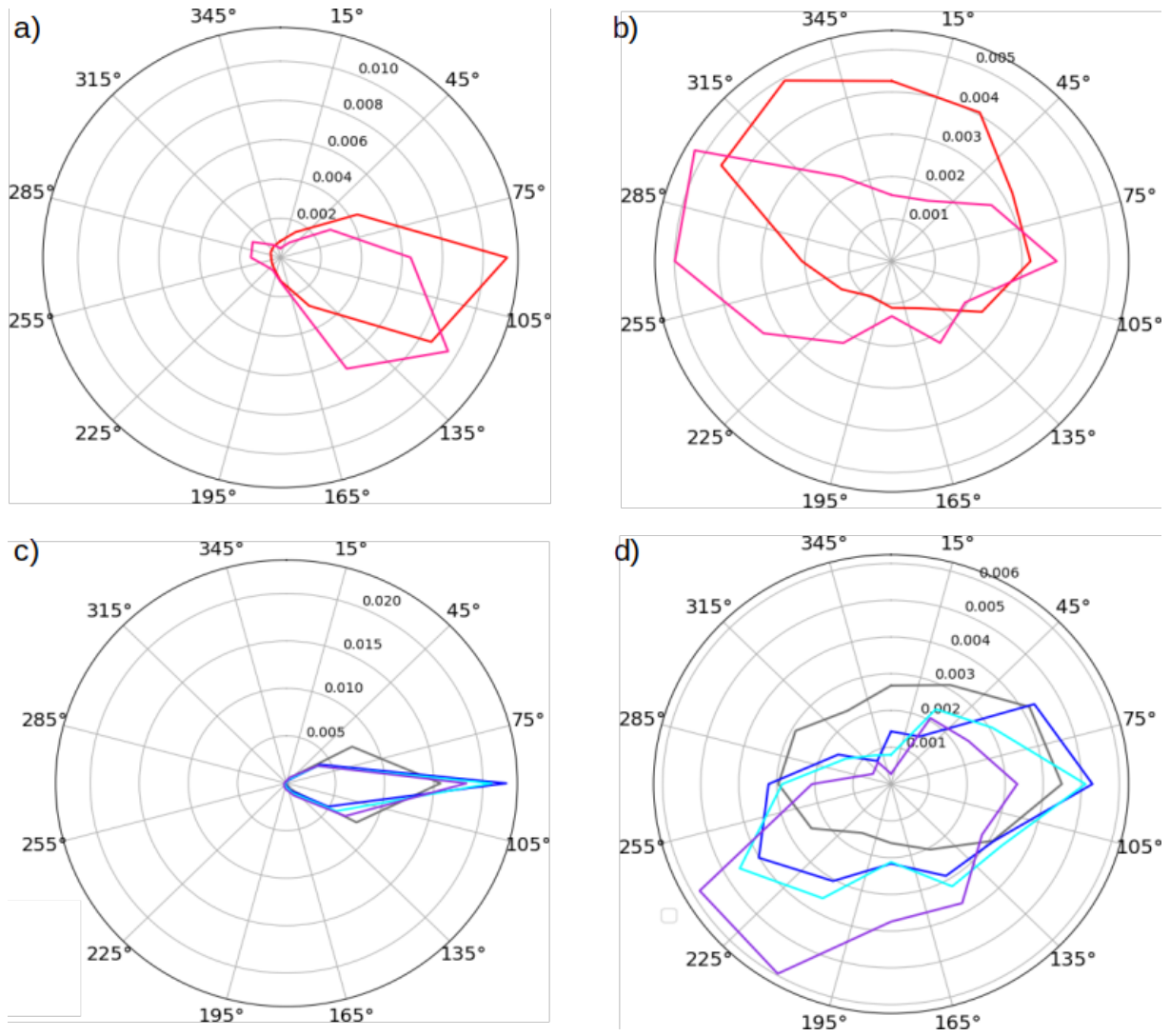


Figure S10. Mean wind rose of 850-hPa wind for each territory (a and b: Reunion and Mayotte; c and d: French West Indies and French Guiana; same colors as Figures 1, 2a, 4a, b). The radius corresponds to the normalized frequency of occurrence within sectors indicated with labels. Left: Climatological wind; right: direction of 850-hPa wind anomaly.

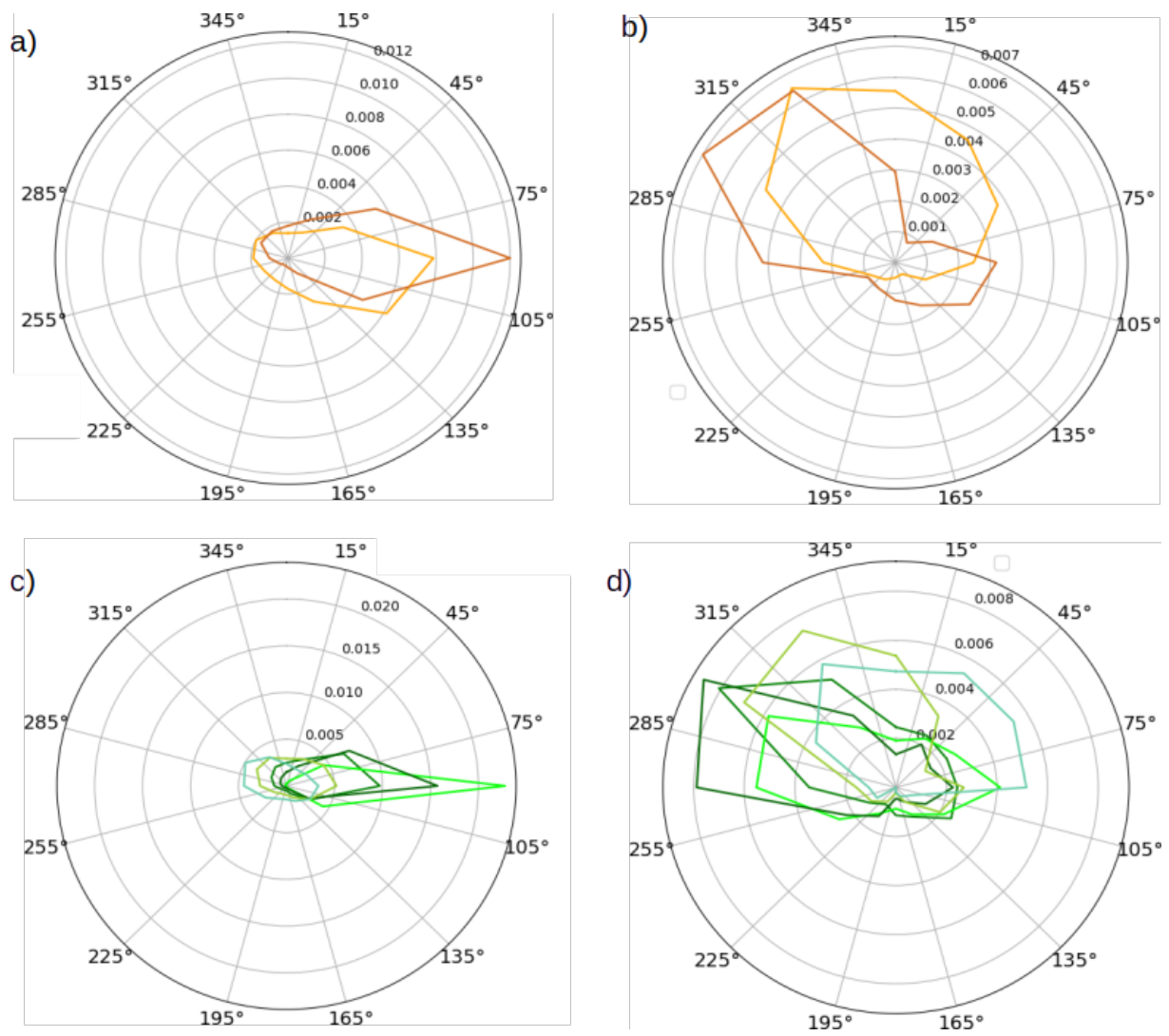


Figure S11. Same as Figure S10 but for New Caledonia and Wallis & Futuna (a,b) and for French Polynesia (c,d)

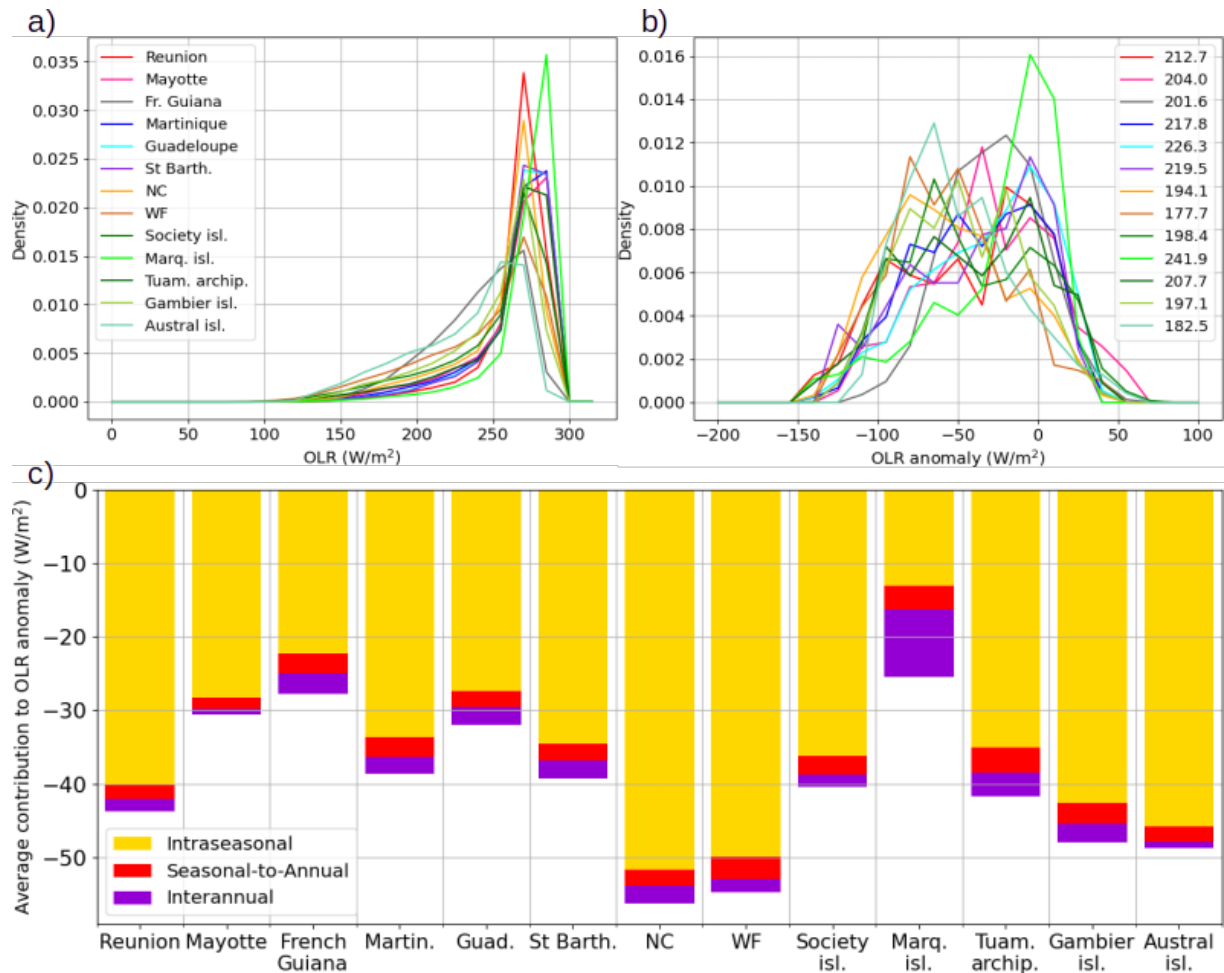


Figure S12. Same as Figure 4 but for OLR. Bins are 15 W m^{-2} wide. In (b), the mean value of OLR during non-cyclonic EPEs is indicated in the legend. These mean values correspond between the 7th percentile (Reunion, NC) and the 15th percentile (French Guiana) of climatological PDFs. About 75% (French Guiana and Mayotte) to 92% (WF) of non-cyclonic EPEs are associated with negative OLR anomalies